Dynamics and Control 2, 147–159 (1992)
© 1992 Kluwer Academic Publishers, Boston. Manufactured in The Netherlands.

On the Flight of a Golf Ball in the Vertical Plane

ROBERT F. STENGEL
Department of Mechanical and Aerospace Engineering, Princeton University, Princeton, NJ 08544

Received July 26, 1990; revised March 26, 1991
Editor: H. Flashner

Abstract. The equations of motion for a ball moving in a vertical plane are used to calculate flight paths for a typical golf ball subjected to a variety of launch conditions, spin rates, atmospheric parameters, and wind fields. Time histories of the ball's velocity, flight-path angle, height, range, and spin rate between tee and first impact illustrate that lift induced by the ball's spin has a significant effect on driving range, actually causing the flight-path angle to increase during the first few seconds of flight. While light winds have the expected effects, heavy tailwind is shown to spoil the carry of the ball. Linearized sensitivity analysis indicates that wind uncertainty is an important contributor to impact range and time uncertainty.

1. Introduction

The flight of golf balls is the focus of considerable attention, not only from the players but from the manufacturers of golfing equipment, the publications and communications media, and the associations that establish and enforce the rules of the game. Not surprisingly, there is a wealth of folklore that has sprung up over the years regarding the effects of various clubs, balls, swings, and environmental effects, but there has been little correlation of these objective factors with the flight of the ball once it has left the tee. Observational data are reported in [1–3], while aerodynamic measurements and rudimentary flight path calculations are shown in [4–7].

In this article, golf-ball flight paths are computed from the tee to first impact, assuming that motion is restricted to a vertical plane. The ball moves up and out along a constant direction once it leaves the tee, without hooks, slices, or crosswind effects. The ball may spin (in fact, substantial backspin is a precondition for a long drive), but the spin axis is assumed to be perpendicular to the plane of motion. These assumptions are consistent with the essential features of the "textbook" drive.

2. Equations of motion

The equations that describe the golf ball's longitudinal motion are readily derived from Newton's Laws of Motion (e.g., [8–9]). They are written in an earth-relative frame of reference, which is assumed to be inertially fixed, and round-earth effects are neglected. There are five solution variables: velocity magnitude (V, ft/sec), flight-path angle (γ, measured from the horizontal, deg), height above the tee (h, ft), horizontal range from the tee (r, ft), and pitching angular rate (q, rpm; backspin is positive). There are five equations of motion that express the time-rates of change, $d(\ )/dt$, for each variable:

$$dV/dt = (L \sin \gamma_w - D \cos \gamma_w)/m - g \sin \gamma, \tag{1}$$

$$d\gamma/dt = [(L \cos \gamma_w + D \sin \gamma_w)/m - g \cos \gamma]V, \tag{2}$$

$$dh/dt = V \sin \gamma, \tag{3}$$

$$dr/dt = V \cos \gamma, \tag{4}$$

$$dq/dt = M/I_{yy}. \tag{5}$$

m is the mass (slugs) of the ball, I_{yy} is its pitching moment of inertia (slug-ft^2), and g is the gravitational constant (32.2 ft/sec^2). In the present case, the ball diameter is taken to be 1.68 in, and its weight is 0.10125 lb; m and I_{yy} are defined accordingly. The terms L, D, and M are aerodynamic left, drag, and pitching moment, respectively, while γ_w is a small angle that accounts for the wind's effect on lift and drag orientation, as discussed below.

The lift and drag forces are expressed as

$$L = C_L QS, \tag{6}$$

$$D = C_D QS. \tag{7}$$

Here, C_L and C_D are nondimensional lift and drag coefficients, Q is the dynamic pressure ($\rho V_a^2/2$, where ρ is the atmospheric density (slugs/ft^3) and V_a is the air-relative velocity (ft/sec), and S is a reference area (ft^2), that is, the frontal area of the sphere. The atmospheric density is a function of air pressure, p (in of mercury), air temperature, T (°F), and relative humidty, μ (%), computed here by the polynomial

$$\rho = a_0 + a_1\Delta p + a_2\Delta T - a_3\Delta\mu + a_4\Delta p\Delta T + a_5\Delta p\Delta\mu + a_6\Delta T\Delta\mu + a_7\Delta p\Delta T\Delta\mu, \tag{8}$$

where

$$\Delta p = p - 29.32 \text{ in. Hg}, \quad \Delta T = T - 100 \text{ °F}, \quad \Delta\mu = 0.01(\mu - 90) \%,$$

and

$$a_0 = 0.00211, \; a_1 = 0.000067, \; a_2 = -0.0000049, \; a_3 = -0.0000533,$$
$$a_4 = -2.6 \times 10\text{-}7, \; a_5 = 2.2 \times 10\text{-}6, \; a_6 = -8.6 \times 10\text{-}7, \; a_7 = 3.0 \times 10\text{-}8.$$

Since the maximum height variation of the ball is a few hundred feet or less, air density is considered to be constant. If the wind is not blowing, the airspeed is the same as the earth-relative speed, $V_a = V$. If there is wind, it adds vectorially to the earth-relative speed

to form the airspeed. Denoting vertical (height) and horizontal (range) components of the wind as w_h and w_r, the vertical and horizontal components of the airspeed are

$$V_{a_h} = V \sin \gamma + w_h, \tag{9}$$

$$V_{a_r} = V \cos \gamma + w_r. \tag{10}$$

Consequently, the airspeed and air-relative flight-path angle are

$$V_a = (V_{a_h}^2 + V_{a_r}^2)^{1/2}, \tag{11}$$

$$\gamma_a = \tan^{-1} (V_{a_h}/V_{a_r}). \tag{12}$$

Lift and drag are defined as forces perpendicular and parallel to the air-relative velocity vector, which is displaced from the earth-relative velocity vector by the angle

$$\gamma_w = \gamma - \gamma_a. \tag{13}$$

This angle (which is zero if there is no wind) must be taken into account when the effects of lift and drag on dV/dt and $d\gamma/dt$ are computed (equations (1) and (2).

C_L and C_D are experimentally determined coefficients that depend on numerous characteristics of the golf ball, e.g., surface roughness, spin rate, and Reynolds number. (Reynolds number is an aerodynamic parameter that portrays the ratio of pressure forces to viscous forces, defined as $V_a d/v$, where d is the ball's diameter and v is the kinematic viscosity coefficient of air.) A generic aerodynamic model of a dimpled golf ball obtained from the United States Golf Association is used here, providing C_L and C_D as tabulated functions of spin rate and Reynolds number.

The aerodynamic pitching moment for a symmetric sphere is modeled as a damping effect that slows the spin of the ball. We use a conventional expression,

$$M = C_{m_q} \rho V_a S d q/4, \tag{14}$$

where C_{m_q} is an empirically derived dimensionless coefficient that is affected by the ball's surface roughness and Reynolds number. In the present work, C_{m_q} has been treated as a selectable fixed parameter. The only effect of pitching moment is to cause the initial spin rate imparted by the driver to decay. This, in turn, affects the flight of the ball through its effect on C_L and C_D (primarily during the early portion of the trajectory, when the aerodynamic forces are greatest).

The nonlinear, ordinary differential equations (1)–(5) are integrated to produce a time history of the ball's flight from the tee to impact. Numerical integration is a sequential process that begins with the initial conditions just after the ball has been hit (V_0, γ_0, h_0, r_0, q_0) and computes the incremental changes in the variables during short intervals of time, Δt. The fourth-order Runge–Kutta algorithm has been used here with $\Delta t = 0.25$ seconds. Computations for each variable depend on the instantaneous values of other variables, so the results are coupled to each other.

3. Results of flight-path computation

A typical trajectory is shown in Figure 1, with $V_0 = 250$ ft/sec, $\gamma_0 = 10°$, $h_0 = r_0 = 0$, $q_0 = 3000$ rpm, and $C_{m_q} = 0$. Because there is no pitch damping, the spin rate remains constant from start to finish. The velocity decreases rapidly coming off the tee, losing almost 70 ft/sec in the first second; it reaches a minimum just over a second beyond its highest point, then increases slightly as the ball drops in. Lift causes the flight-path angle (γ) to increase almost 3° coming off the tee, counteracting the force of gravity during that time. The ball has traveled two thirds of its total range by the time it reaches its peak altitude (105 ft), and it follows a steeper path in descent than during ascent. The Reynolds number increases from "supercritical" ($>100{,}000$) to "subcritical" ($<100{,}000$) values just prior to the trajectory's peak. (C_L and C_D tend to be larger in the supercritical region.) The ball travels 270 yd in 7 sec, impacting at an angle of about −45°.

Figure 2 illustrates the effects of initial flight-path angle on the height vs. range profile. The initial velocity is 230 ft/sec, there is no wind or pitch damping, and the air is hot and humid. The maximum height continues to increase as γ_0 increases from 10° to 30°, and the maximum range is achieved for launch angles between 20° and 30°. (For the cases shown, the 20° impact range is slightly greater than the 30° range.) Aerodynamic lift produces an upward curvature in the path that contributes to increased height, flight time, and impact range.

The maximum range actually occurs for $\gamma_0 = 25°$ (Figure 3). With launch velocity held constant, the maximum occurs when the effects of the increasing flight time are just balanced by the effects of decreasing groundspeed (horizontal earth-relative speed) with increasing launch angle. Although the range change in this launch-angle region is small, there is a monotonic increase in impact time with increasing launch angle.

With launch angle held constant at 10°, variations in launch velocity from 200 to 300 ft/sec produce the impact results shown in Figure 4. Increases in impact range and time are linearly related to launch velocity.

Variations in the fixed spin rate from 0 to 3600 rpm affect the impact point, as shown in Figure 5. Impact range and time increase almost linearly as spin rate increases from 0 to 1000 rpm, reflecting the growing lift. The spin effect on range plateaus for spin rates above 2000 rpm, although impact time continues to increase.

Arbitrary independent variations in lift and drag magnitude produce expectable trends in impact range and time, although the relative sizes of these effects may be unanticipated (Figure 6). For this series of runs, initial velocity is 230 ft/sec, launch angle is 10°, and pressure, temperature, and humidity are 29.92 in. Hg, 59°F, and 30%, respectively. Pitch damping (−0.0025) causes the spin rate to decrease from 3000 rpm to about 2000 rpm during the time of flight. (This level of damping reduces impact range by about 4 ft, in comparison to the constant-spin-rate case.) In each case, the lift (or drag) coefficient obtained from table lookup was multiplied by a constant between 0.9 and 1.1. A 10% drag increase has a more significant effect on range that a 10% lift decrease; however, their effects on impact time are more nearly equal. A combined increase in lift and drag is dynamically equivalent to an increase in the reference area (proportional to ball diameter-squared) or a mass decrease of the same percentage.

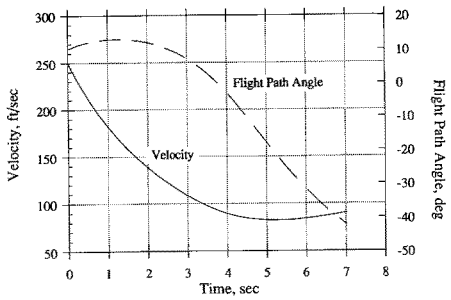

a) Velocity and flight path angle vs. time;

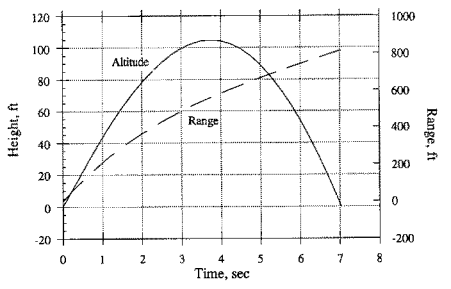

b) altitude and range vs. time;

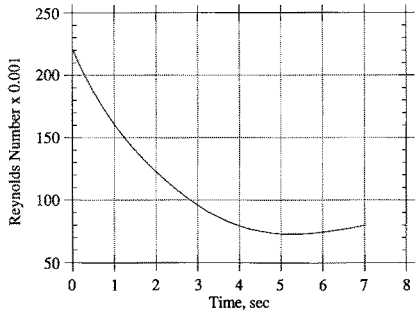

c) Reynolds number vs. time.

Figure 1. Trajectory of a typical drive, with initial velocity = 250 ft/sec and initial flight path angle = 10°.

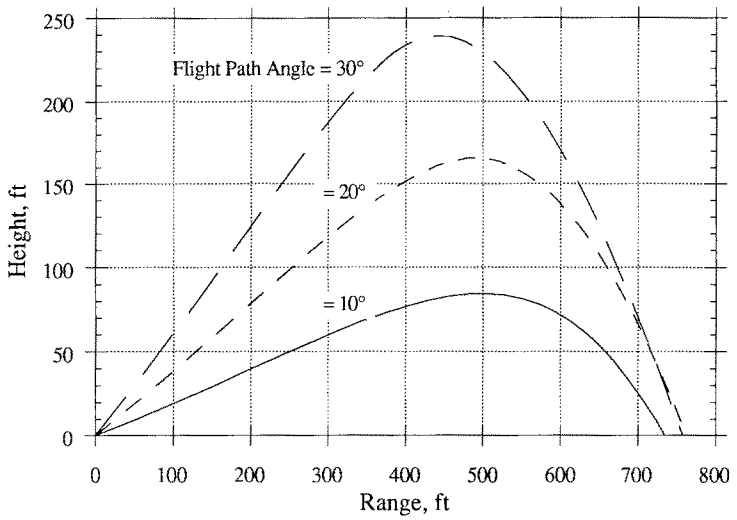

Figure 2. Typical flight paths for three launch angles. Initial velocity = 230 ft/sec.

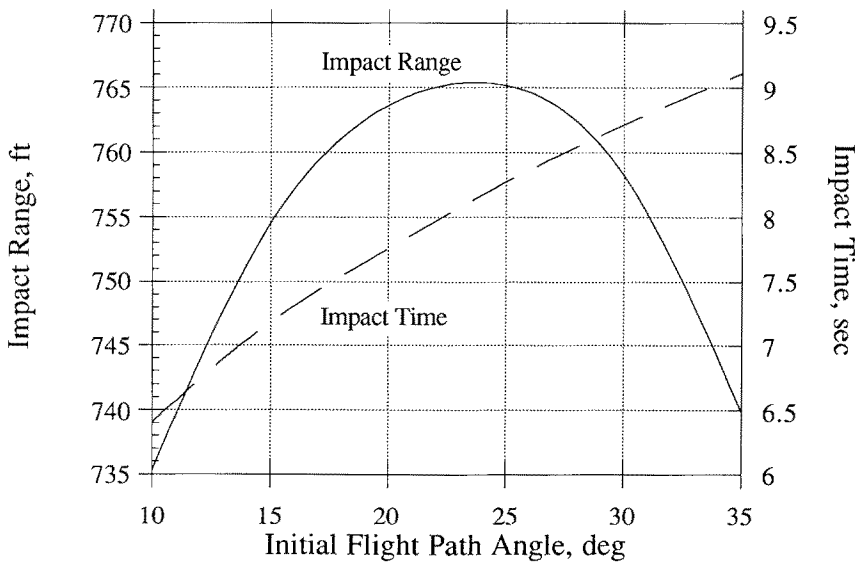

Figure 3. Effect of initial flight-path angle on impact range and time. Initial velocity = 230 ft/sec.

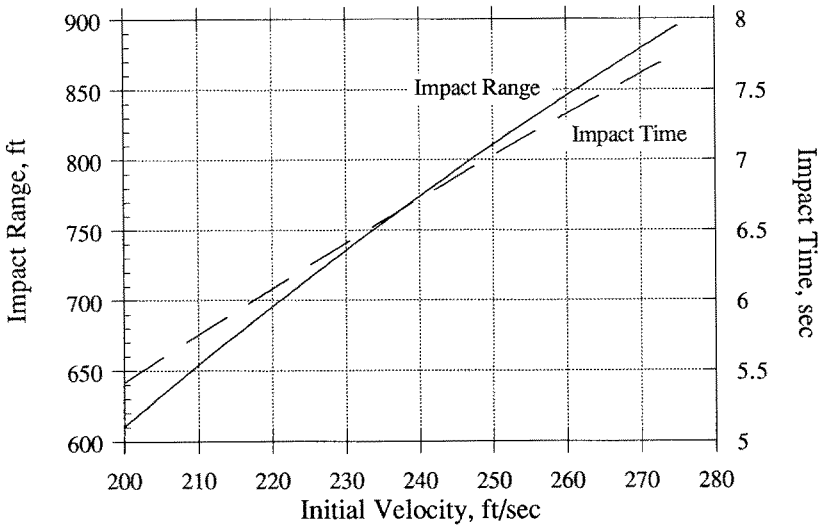

Figure 4. Effect of launch velocity on impact range and time. Initial flight-path angle = 10°.

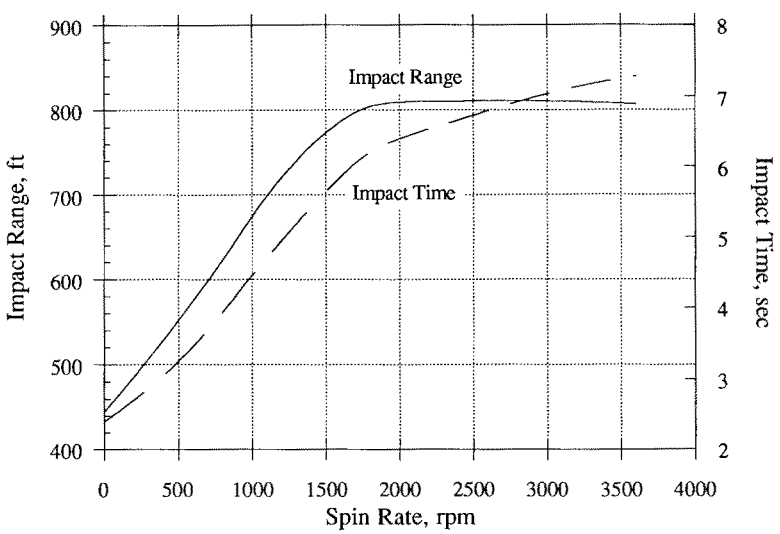

Figure 5. Effect of spin rate on impact range and time. Initial velocity = 250 ft/sec. Initial flight-path angle = 10°.

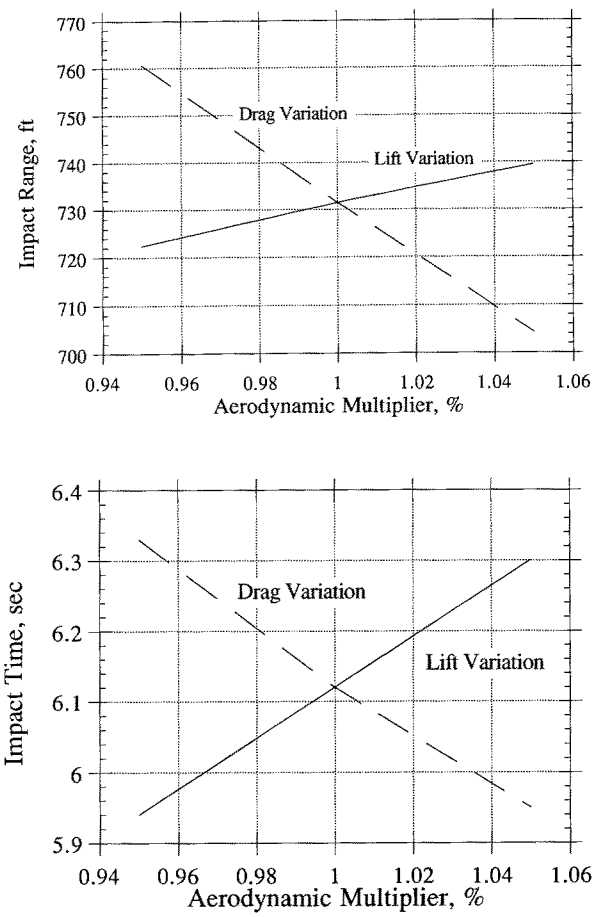

Figure 6. Effects of lift and drag variations on impact range and time. Initial velocity = 230 ft/sec. Initial flight-path angle = 10°. Pitch damping derivative = −0.0025. a) Impact range variation; b) impact time variation.

Constant head/tailwind effects produce an unexpected result that, nevertheless, is consistent with golfing folklore. As Figure 7 shows, winds ranging from −80 ft/sec (tailwind) to +80 ft/sec (headwind) have an absolutely linear effect on impact time, increasing the time of flight through lift-induced lofting of the trajectory. Increasing headwind decreases the carry substantially, and modest tailwinds increase range. However, strong tailwinds (above 45 ft/sec) decrease the range by spoiling lift. Reduced maximum height and impact time conspire to shorten the drive.

4. Linear sensitivities to parametric variations

Although impact range and time have nonlinear relationships to large variations in several of the parameters discussed above, the sensitivities to small variations in the neighborhood

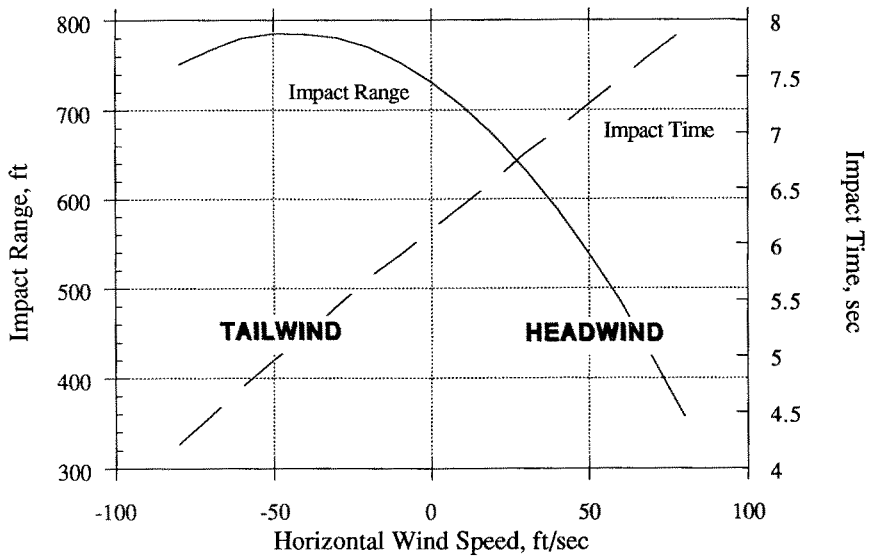

Figure 7. Effect of head/tailwind on impact range and time. Initial velocity = 230 ft/sec. Initial flight-path angle = 10°. Pitch damping derivative = −0.0025.

of given nominal conditions are well approximated as linear. For example, a unit change in launch velocity causes a change of Δr feet in impact range and Δt seconds in impact time; in the limit, this sensitivity is expressed by a partial derivative. In the current example, the impact range sensitivity is symbolized as $\partial r_f/\partial V_0$, and the impact time is denoted by dt_f/dV_0, where the subscripts indicate final and initial values. For small perturbations, the effects are additive; thus, known launch velocity and angle perturbations of ΔV_0 and $\Delta\gamma_0$ cause impact range and time variations that are well approximated by

$$\Delta r_f \approx (\partial r_f/\partial V_0)\Delta V_0 + (\partial r_f/\partial \gamma_0)\Delta\gamma_0, \tag{15}$$

$$\Delta t_f \approx (\partial t_f/\partial V_0)\Delta V_0 + (\partial t_f/\Delta\gamma_0)\Delta\gamma_0, \tag{16}$$

and the effect of other known variations in the conditions of the ball's flight can be added accordingly.

A number of linear sensitivity coefficients are given in the remainder of this section. They were calculated by differencing numerical results with the assumption that initial velocity is 230 ft/sec, launch angle is 10°, initial spin rate is 3000 rpm, pitch damping (C_{m_q}) is −0.0025, and pressure, temperature, and humidity are 29.92 in. Hg, 59°F, and 30%, respectively. The nominal impact range and time are 731.47 ft and 6.13 sec.

Atmospheric pressure effect

$$\partial r_f/\partial p = -3.95 \text{ ft/in. Hg}, \quad \partial t_f/\partial p = 0.05 \text{ sec/in. Hg}$$

Air temperature effect

$$dr_f/\partial T = 0.26 \text{ ft/°F}, \; \partial t_f/\partial T = -0.0004 \text{ sec/°F}$$

Humidity effect

$$\partial r_f/\partial \mu = 0.0033 \text{ ft/\%}, \; \partial t_f/\partial \mu = -0.0003 \text{ sec/\%}$$

Initial velocity effect

$$dr_f/\partial V_0 = 3.96 \text{ ft/(ft/sec)}, \; \partial t_f/\partial V_0 = 0.029 \text{ sec/(ft/sec)}$$

Initial flight-path-angle effect

$$\partial r_f/\partial \gamma_0 = 5.81 \text{ ft/deg}, \; \partial t_f/\partial \gamma_0 = 0.16 \text{ sec/deg}$$

Initial spin-rate effect

$$\partial r_f/\partial (\text{rpm})_0 = -0.0095 \text{ ft/rpm}, \; \partial t_f/\partial (\text{rpm})_0 = 0.00032 \text{ sec/rpm}$$

Lift magnitude effect

$$\partial r_f/\partial L = 1.71 \text{ ft/\%}, \; \partial t_f/\partial L = 0.036 \text{ sec/\%}$$

Drag magnitude effect

$$\partial r_f/\partial D = -5.64 \text{ ft/\%}, \; \partial t_f/\partial D = -0.038 \text{ sec/\%}$$

Horizontal wind effect

$$\partial t_f/\partial w_r = -2.47 \text{ ft/(ft/sec) (headwind)}, \; \partial t_f/\partial w_r = 0.023 \text{ sec/(ft/sec)}$$

Vertical wind effect

$$\partial r_f/\partial w_h = -6.116 \text{ ft/(ft/sec) (downdraft)}, \; \partial t_f/\partial w_h = -0.066 \text{ (sec/(ft/sec)}$$

5. Linearized uncertainty analysis

The linearized sensitivity analysis predicts the effects of known parametric variations. When the parametric variations are random, the effect of multiple variations combine in different ways, depending on the degree to which these variations are correlated. Rather then considering deterministic variations in range and time, Δr_f and Δt_f, we want to know the *standard deviations* of these quantities, σ_r and σ_t.

Three cases are interesting: multiple variations are perfectly correlated, multiple variations are perfectly uncorrelated, and two variations are precisely "anticorrelated." For the linear case, the standard deviations of two perfectly correlated variables, σ_y and σ_x, are related by

$$\sigma_y = |\partial y/\partial x|\sigma_x, \tag{17}$$

where $|\partial y/\partial x|$ is the absolute value of the partial derivative referred to previously. If two correlated random variables, x_1 and x_2, affect y, σ_y is the sum of the absolute values of their effects; if x_1 and x_2 are anticorrelated, their effect is the absolute value of their difference. If they are perfectly uncorrelated, they have a root-sum-square effect, i.e.,

$$\sigma y = \{[(\partial y/\partial x_1)\sigma_1]^2 + [(\partial y/\partial x_2)\sigma_2]^2\}^{1/2} \tag{18}$$

and this formula can be extended to include the effects of more than two variables. In all cases, we can use the sensitivities derived in the previous section.

Consider the three alternatives in evaluating the effects of lift and drag uncertainty. Assume that the percentage uncertainties in lift and drag coefficients are equal, e.g., 1% of their estimated values. For a normal (Gaussian) probability distribution, there is a 68% chance that C_L and C_D are within 1% of their assumed values, but we do not know their values precisely. If there is no reason to believe that the lift and drag uncertainties are correlated, then the impact range and time standard deviations are estimated as

$$\sigma_r = (1.71^2 + 5.64^2)^{1/2}\sigma = 5.89\sigma \text{ft}, \tag{19}$$

$$\sigma_t = (0.036^2 + 0.038^2)^{1/2}\sigma = 0.052\sigma \text{ sec}, \tag{20}$$

where σ is the standard deviation of both C_L and C_D. For the normal distribution, there is a 94% chance of impacting within twice this spread and a 99% chance of landing within three times this spread.

If lift and drag estimation errors are correlated so that 1% lift increase corresponds to 1% drag increase, the effects tend to cancel (Figure 5); hence,

$$\sigma_r = |5.64 - 1.71|\sigma = 3.93\sigma \text{ft}, \tag{21}$$

$$\sigma_t = |0.038 - 0.036|\sigma = 0.02\sigma \text{sec}. \tag{22}$$

If measurement errors are correlated so that lift increases correspond to drag decreases, the effect on impact range and time are additive; therefore,

$$\sigma_r = |1.71 + 5.64|\sigma = 7.35\sigma \text{ft}, \tag{23}$$

$$\sigma_t = |0.036 + 0.038|\sigma = 0.0074\sigma \text{sec}. \tag{24}$$

A similar assessment of launch condition uncertainties can be conducted. Using the sensitivites of the previous section, we obtain the combined effects shown in Table 1. Here,

Table 1. Effect of launch uncertainties on impact uncertainties.

	Uncorrelated	Correlated	Anticorrelated
σ_r, ft	4.	4.54	3.38
σ_t, sec	0.033	0.045	0.013

it is assumed that the velocity standard deviation is 1 ft/sec and the launch-angle standard deviation is 0.1°, values that are considerably smaller than most golfers could achieve but that are representative of the launch accuracy of a well-calibrated "mechanical golfer.'

Comparing the impact condition uncertainties that result from temperature, pressure, humidity, and wind, it is clear that the last of these has dominant effect (for reasonable standard deviations). Given a 5-ft/sec uncertainty in the head/tailwind, a 12.4-ft impact range uncertainty and 0.12-sec impact time uncertainty could be anticipated. Adding an uncorrelated 5-ft/sec uncertainty in the vertical wind increases the impact time uncertainty to 0.35 sec and the impact range uncertainty to 33 ft. If we root-sum-square these figures with the effects of launch condition uncertainty (there is no reason to expect them to be correlated), we find that the impact range uncertainty is 33.2 ft, while the impact time uncertainty is 0.35 sec. Once again, the wind uncertainty is seen to be the dominant factor.

6. Conclusion

The dynamic equations describing the flight of a golf ball in the vertical plane have been used to conduct an analysis of the effects of several parameters on impact range and time. In addition to providing details of the trajectory, these results establish a basis for linear sensitivity analyses, including the assessment of uncertainties associated with experiments on the driving range and in the wind tunnel. An informal comparison with driving range tests suggests that the computed results are accurate. Lift induced by the ball's spin has a significant effect on driving range, actually causing the flight path angle to increase during the first few seconds of flight. While light winds have the expected effects, heavy tailwind is shown to spoil the carry of the ball. Linearized sensitivity analysis indicates that wind uncertainty is an important contributor to impact range and time uncertainty.

Acknowledgment

This research was sponsored by the United States Golf Association, Far Hills, New Jersey.

References

1. P.G. Tait, "Some points in the physics of golf, part I," *Nature,* vol. 42, pp. 420–423, 1890.
2. P.G. Tait, "Some points in the physics of golf, part II," *Nature,* vol. 44, pp. 497–498, 1891.
3. P.G. Tait, "Some points in the physics of golf, part III," *Nature,* vol. 48, pp. 202–205, 1893.

4. J.M. Davies, "The aerodynamics of golf balls," *J. Appl. Phys.*, vol. 20, pp. 821–828, 1949.
5. P.W. Bearman and J.K. Harvey, "Golf ball aerodynamics," *Aeronaut. Q.* vol. 27, pp. 112–122, 1976.
6. R.D. Mehta, "Aerodynamics of sports balls," *Ann. Rev. Fluid Mech.* vol. 17, pp. 151–189, 1985.
7. Y. Nakayama, K. Aoki, and M. Kato, "Flow visualization around golf balls," *Proc. Fourth Int. Symp. on Flow Visualization*, Paris, 1986, pp. 191–196.
8. A. Miele, *Flight Mechanics, Volume 1: Theory of Flight Paths.* Addison-Wesley: Reading, MA, 1962.
9. R.F. Stengel and P. Berry, "Stability and Control of Maneuvering High-Performance Aircraft," NASA CR-2788, Washington, DC, 1977.